Int. J. Electrochem. Sci., 7 **(2012)** 4847 - 4859

International Journal of
ELECTROCHEMICAL
SCIENCE
www.electrochemsci.org

Effects of 3-Amino-1,2,4-triazole-5-thiol on the Inhibition of Pure Aluminum Corrosion in Aerated Stagnant 3.5 wt.% NaCl Solution as a Corrosion Inhibitor

El-Sayed M. Sherif [1,2,*]

[1] Center of Excellence for Research in Engineering Materials (CEREM), College of Engineering, King Saud University, P. O. Box 800, Al-Riyadh 11421, Saudi Arabia
[2] Electrochemistry and Corrosion Laboratory, Department of Physical Chemistry, National Research Centre (NRC), Dokki, 12622 Cairo, Egypt
E-mail: esherif@ksu.edu.sa

Received: 24 April 2012 / *Accepted:* 18 May 2012 / *Published:* 1 June 2012

Aluminum and its alloys are widely used in so many applications owing to their important characteristics. The use of aluminum gets limited due to its corrosion when exposed to aggressive environments, especially those containing chloride ions. In this work, the effects of 3-amino-1,2,4-triazole-5-thiol (ATAT) on the inhibition of unalloyed aluminum of corrosion in aerated stagnant 3.5 wt.% NaCl solution as a corrosion inhibitor was studied. Cyclic potentiodynamic polarization (CPP), potentiostatic current-time (CCT), and electrochemical impedance spectroscopy (EIS) were employed. CPP measurements showed that Al in 3.5 wt.% NaCl suffers both uniform and pitting corrosion; the presence of ATAT and the increase of its concentrations inhibit this corrosion by decreasing the corrosion current and corrosion rate and increasing the polarization resistance of Al. The CCT experiments at -680 mV vs. Ag/AgCl indicated that ATAT decreases the absolute current values for Al. EIS data concluded that the surface and charge transfer resistances for Al increase by the addition and upon the increase of ATAT concentration.

Keywords: 3-Amino-1,2,4-triazole-5-thiol, aluminum, corrosion inhibition, cyclic polarization, impedance, 3.5 wt.% NaCl solutions

1. INTRODUCTION

Aluminum metal is characterized by its good electrical and thermal conductivities, high strength to weight ratio, easy to deform, high ductility, and good corrosion resistance [1,2]. For this, it is widely used as a material in manufacturing automobile and aircraft components due to its high

strength to weight ratio in order to make the moving vehicle lighter, which results in saving in fuel consumption, household appliances, aviation, containers, etc [3-5]. It is generally believed that aluminum forms a compact, strongly adherent and continuous film if it is exposed to the atmosphere [6,7]. However, this oxide film may dissolve and different forms of aluminum corrosion take place in many environments including those containing chloride ions [1-4,8,9].

Under these circumstances, corrosion inhibitors are considered for possible aluminum protection against corrosion in the corrosive environments, which is why numerous studies have been conducted by several researchers to find powerful corrosion inhibitors for aluminum in those media [1,2,10–17]. This includes the use of either inorganic oxidants such as chromate, molybdate and tungstate [10-13], or organic corrosion inhibitors [1,2,14-17]. Heterocyclic compounds having oxygen, sulfur, and/or nitrogen as polar groups, and other organic compounds containing functional groups and conjugated double bonds have been reported to be good corrosion inhibitors [1,2,14-17]. The efficiency of these compounds as corrosion inhibitors results from their adsorption onto the metal surface. This is usually done by chemisorptions, physisorption, or complexation of the metal with the polar groups, which are regarded as the reactive centers in the organic molecules.

The aim of the current study was to report the effects of ATAT molecules on the corrosion inhibition of unalloyed aluminum in aerated stagnant 3.5 wt.% sodium chloride solutions using variety of conventional electrochemical techniques and electrochemical impedance. ATAT has been proven a powerful inhibition effectiveness on the inhibition of iron [18] and copper [19-22] in chloride media. It was anticipated that ATAT would have a good inhibition efficiency for aluminum in the aerated stagnant 3.5 wt.% NaCl solution because it is a heterocyclic compound containing there azole groups, an amino group and a mercapto group. The presence of these groups allows the ATAT molecules to be adsorbed on the aluminum surface to prevent the formation of aluminum chlorides, $AlCl_3$, or chloride complexes, $AlCl_4^-$ or other soluble oxychloride complexes, $Al(OH)_2Cl_2^-$, which lead to Al corrosion as has been reported in our previous studies [1,2,4,8]. In addition, ATAT is nontoxic and inexpensive compound compared with many other organic compounds.

2. EXPERIMENTAL PROCEDURE

Sodium chloride (NaCl) with 99% purity was obtained from Merck Chemicals. 3-Amino-1,2,4-triazole-5-thiol (ATAT) with 95% purity was purchased from Sigma–Aldrich Corporation. N,N-Dimethylfomamide ((DMF), was purchased from WinLab at Wilfrid Smith Limited (Middlesex, UK)). All these chemical compounds were used as received. A 70 gm NaCl was weighed and dissolved in doubly-distilled water to both complete a 1000 ml glass measuring flask; this forms a stock of 7 wit.% NaCl solution. The 3.5 wt.% NaCl solution was prepared from the stock solution by dilution.

An electrochemical cell with a three-electrode configuration was used; an aluminum rod (Al, Aldrich, 99.99% in purity, 6.5 mm in diameter), a platinum foil, and an Ag/AgCl electrode (in the saturated KCl) were used as the working, counter, and reference electrodes, respectively. The Al rod for electrochemical measurements was prepared by welding a copper wire to a drilled hole was made on one face of the rod; the rod with the attached wire were then cold mounted in resin and left to dry in

air for 24 h at room temperature. Before measurements, the other face of the Al electrode, which was not drilled, was first grinded successively with metallographic emery paper of increasing fineness up to 800 grit and further polished with 5, 1, 0.5, and 0.3 mm alumina slurries (Buehler). The electrode was then cleaned using doubly-distilled water, degreased with acetone, washed using doubly-distilled water again and finally dried with dry air.

An Autolab Potentiostat (PGSTAT20 computer controlled) operated by the general purpose electrochemical software (GPES) version 4.9 was used to perform the electrochemical experiments. The cyclic polarization (CPP) curves were obtained by scanning the potential in the forward direction from -1800 to -500 mV against Ag/AgCl at a scan rate of 3.0 mV/s; the potential was then reversed in the backward direction at the same scan rate. Chronoamperometric current-time (CT) experiments were carried out by stepping the potential of the aluminum samples at – 680 mV versus Ag/AgCl for 60 minutes. Impedance (EIS) tests were performed at corrosion potentials (EOCP) over a frequency range of 100 kHz – 100 mHz, with an ac wave of ± 5 mV peak-to-peak overlaid on a dc bias potential, and the impedance data were collected using Powersine software at a rate of 10 points per decade change in frequency.

All the electrochemical experiments were carried out at room temperature in freely aerated solutions consist of 98/2 : vo/vol : water/DMF.

3. RESULTS AND DISCUSSION

3.1. Cyclic potentiodynamic polarization (CPP) measurements

In order to obtain the corrosion parameters and to report the effects of ATAT on the inhibition of Al uniform and pitting corrosion in 3.5 wt.% NaCl solutions, CPP measurements were carried out. Fig. 1 shows the CPP curves obtained for Al after 60 min immersion in aerated stagnant 3.5 wt.% NaCl solutions that contain (a) 0.0 mM ATAT, (b) 1.0 mM ATAT and (c) 5.0 mM ATAT, respectively. The values of E_{Corr}, j_{Corr}, cathodic Tafel slope (β_c), anodic Tafel slope (βa), passivation current (j_{Pass}), pitting potential (E_{Pit}), polarization resistance (R_P), corrosion rate (K_{Corr}), and the percentage of the inhibition efficiency (IE%) for ATAT obtained from the polarization curves shown in Fig. 1 for Al, after 60 min immersion in 3.5 wt.% NaCl solutions, are listed in Table 1. The values of the E_{Corr} and j_{Corr} were obtained from the extrapolation of anodic and cathodic Tafel lines located next to the linearized current regions. The j_{Pit} was determined from the forward anodic polarization curves where a stable increase in the current density occurs. The values of K_{Corr}, R_P, and IE% were calculated as has been previously reported [23-29].

It is well known that aluminum develops an oxide film on its surface when exposed to near neutral aerated solutions on two steps according to the following reactions [1, 2,4,8],

$$Al_{(S.)ads.} + 3OH^- = Al(OH)_{3,ads.} + 3e^- \quad (1)$$

$$2Al(OH)_{3,ads.} = Al_2O_3 \cdot 3H_2O \quad (2)$$

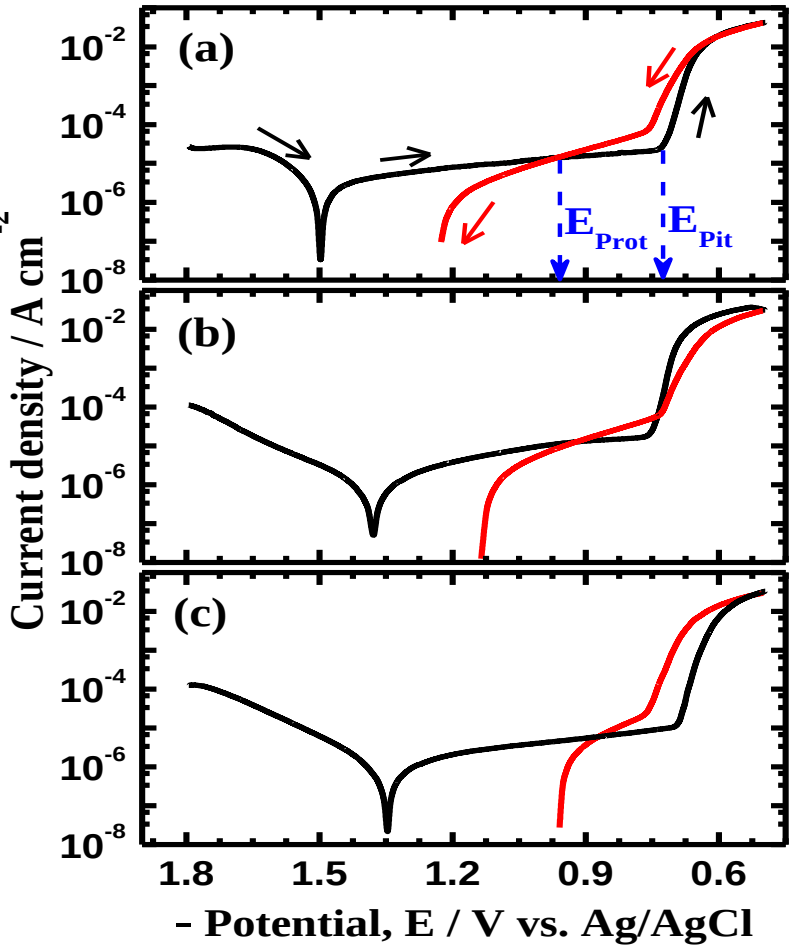

Figure 1. Cyclic potentiodynamic polarization curves obtained for Al after 60 min immersion in aerated stagnant 3.5 wt.% NaCl solutions that contain (a) 0.0 mM ATAT, (b) 1.0 mM ATAT and (c) 5.0 mM ATAT, respectively.

In the presence of corrosive species such as chloride ions, pitting corrosion occurs due to the breakdown of the formed oxide film [30]. Where, the chloride ions attack the weak parts of the oxide film and reach the aluminum surface to produced aluminum chloride complex as follows,

$$Al^{3+} + 4Cl^{-} = AlCl_4^{-} \quad (3)$$

The dissolution of Al(0) to Al(III) under the influence of the chloride ions and the negative potential that is applied on the aluminum surface as follows [1,2,30];

$$Al = Al^{3+} + 3e^{-} \quad (4)$$

On the other hand, the cathodic reaction for metals and alloys in near neutral chloride solutions is the oxygen reduction as has been early reported according to the following reaction [31-36];

$$\frac{1}{2}O_2 + H_2O_{(S)} + e^{-} = OH_{ads.} + OH^{-} \quad (5)$$

The adsorbed hydroxide species further reduced to be in the solution as shown by this Eq.,

$$OH_{ads.} + e^{-} = OH^{-} \quad (6)$$

Table 1. Parameters obtained from cyclic potentiodynamic polarization curves shown in Fig. 1 for the Al electrode in aerated stagnant 3.5 wt.% NaCl solutions in absence and presence of 1 and 5 mM ATAT.

Solution	Parameter								
	βc / mV dec_{-1}	E_{Corr} / mV	j_{Corr} / μA cm^{-2}	βa / mV dec^{-1}	j_{Pass} / μA cm^{-2}	E_{Pit} / mV	Rp / Ω cm^2	K_{Corr} / mmy^{-1}	IE / %
3.5 wt.% NaCl	140	-1485	2.0	165	4.52	-735	16463	0.0218	─
+ 1.0 mM ATAT	105	-1395	0.6	180	3.14	-725	48100	0.0065	70.2
+ 5.0 mM ATAT	92	-1355	0.42	207	1.49	-690	65927	0.0046	78.9

The anodic branch of Al in 3.5 wt% NaCl solution in the absence of any ATAT, Fig. 1 (curve a) shows a large passive region due to the formation of aluminum oxide, Al_2O_3, as indicated by Eq. (1) and Eq. (2). This film does not last under the influence of the increased applied potential to the less negative values. Due to the presence of the chloride ions in a high concentration, 3.5 wt.%, the breakdown of the formed film occurs accompanied by an abrupt increase in the Al current values. This leads to the occurrence of Al pitting corrosion, where the chloride ions attack the flawed regions on the surface oxide film allowing Al to dissolve to Al cations, Al^{3+}, as shown by Eq. (4), which then reacts with the chloride ions from the solution to form $AlCl_3$ and further $AlCl_4^-$, Eq. (3). The later complex compound diffuses into the bulk of the solution allowing the pitting corrosion to occur [37-40]. The chloride ions may work by adsorption onto the aluminum surface and then react with Al(III) that is existed in the aluminum oxide lattice and form an oxychloride complex, $Al(OH)_2Cl_2^-$, Eq. (7). This complex is soluble and its formation increases the anodic dissolution of Al by decreasing the chemical inertness of the natural aluminum oxide film [37-40].

$$Al^{3+}_{(\text{in crystal lattice of the oxide})} + 2Cl^- + 2OH^- = Al(OH)_2Cl_2^- \quad (7)$$

In the presence and upon the increase of ATAT concentration and as can be seen from curve (b) and curve (c) of Fig. 1 and also from the parameters listed in Table 1 that the values of j_{Corr}, j_{Pass} and K_{Corr} decreased and the values of Rp increased. This effect shifted also the values of E_{Corr} and E_{Pit} of Al towards the less negative direction. The value of IE% obtained for Al by ATAT recorded about 70% with 1.0 mM increased to almost 79% with increasing the ATAT concentration to 5.0 mM. This indicates that the presence of ATAT decreases the corrosion of Al in the chloride solution, which is might be due to the adsorption of ATAT molecules onto the Al surface to repairing the flawed areas of the oxide film and preventing the formation of aluminum chloride and oxychloride complexes. It has been reported by Sherif and Park [1, 2] and Yamaguchi and Yamamoto [41] in their studies on the inhibition of Al corrosion by some organic compounds that the inhibition of Al corrosion takes place via the adsorption of these compounds then the formation of a complex with the oxide film of the

aluminum surface. This in turn leads to the formation of Al-O bond, which stabilizes the oxide film and reduces the corrosion of Al.

3.2. Potentiostatic current-time (CCT) measurements

The CCT experiments were performed to see the change of Al currents with time at constant potential value, which was chosen from the CPP curves to be in the anodic active region. The CCT curves obtained at –680 mV (Ag/AgCl) for Al electrode after its immersion for 60 min in aerated stagnant 3.5 wt.% NaCl solutions that contain (1) 0.0 mM, (2) 1.0 mM, and (3) 5.0 mM ATAT, respectively are shown in Fig. 2. The current of Al in the chloride solution alone shows an initial increase due to the dissolution of the flawed parts of the oxide film that was formed on aluminum in chloride solution, which was before stepping the potential to -680 mV vs. Ag/AgCl. The current rapidly decreased in the first few minutes after which the current slowly decreased with some fluctuations until the end of the time of the experiment. The rapid current decreases resulted due to the formation of a corrosion product layer and/or stabilizing the formed oxide film on the electrode surface. The slow decreases in current and its fluctuations resulted from the equilibrium between the initiation of small pits and its blocking by the thickening of Al_2O_3 and/or the accumulation of corrosion products.

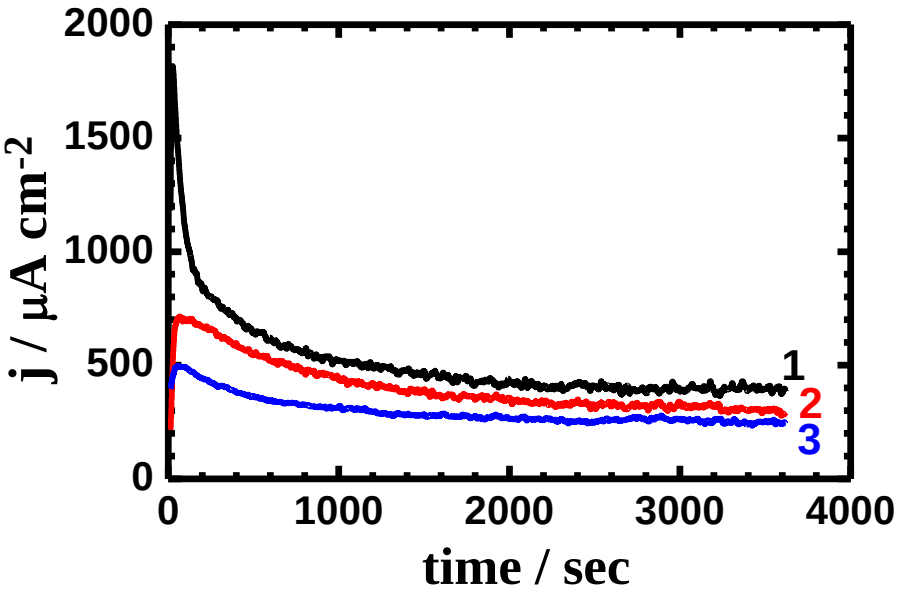

Figure 2. Potentiostatic current-time curves obtained at –680 mV (Ag/AgCl) for Al electrode after its immersion for 60 min in aerated stagnant 3.5 wt.% NaCl solutions containing (1) 0.0 mM, (2) 1.0 mM, and (3) 5.0 mM ATAT, respectively.

The addition of 1.0 mM ATAT to the chloride solution, Fig. 2 curve 2, decreased the initial and absolute currents of Al over the whole time of the experiment. Where, the current started at ~ 200 μAcm^{-2} increased to about 700 μAcm^{-2} in the first few moments after which the current decreased

reaching ~ 300 μAcm^{-2} in 60 min time. It is noticed also that the intensity of current fluctuations almost disappeared. This means that the presence of ATAT decreased both the uniform and initiated pitting corrosion of Al. Increasing the concentration of ATAT to 5.0 mM, Fig. 2 curve 3, further decreased the current of Al to the lowest recorded values, which proves that the ability of ATAT as a corrosion inhibitor increases with increasing its concentration.

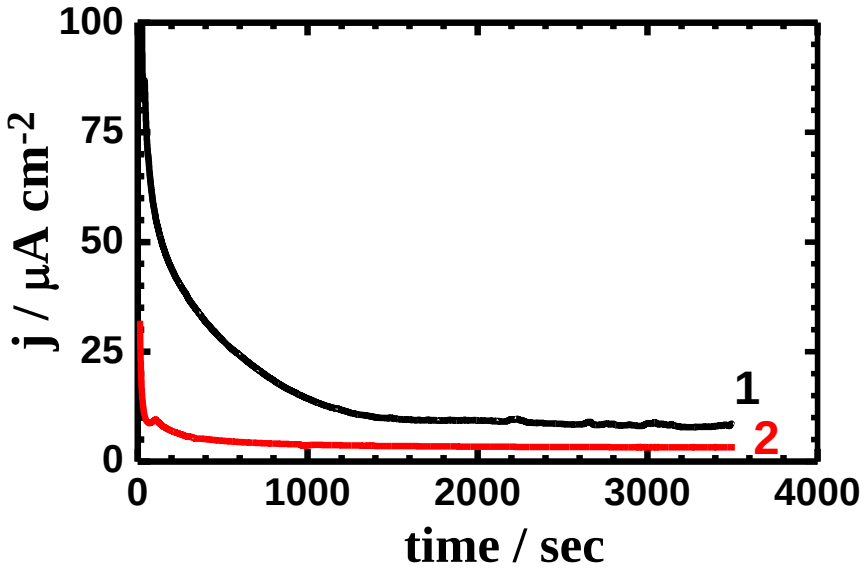

Figure 3. Potentiostatic current-time curves obtained at –680 mV (Ag/AgCl) for Al electrode after its immersion for 10 days in aerated stagnant 3.5 wt.% NaCl solution containing (1) 0.0 and (2) 1.0 mM ATAT, respectively.

In order to shed more light on the effect of ATAT on the current-time behavior for Al after long exposure period, the CCT curves were recorded after 10 days. Fig. 3 shows the CCT curves obtained at -680 mV (Ag/AgCl) for Al electrode after its immersion for 10 days in aerated stagnant 3.5 wt.% NaCl solution in the absence (1) and in the presence of (2) 1.0 mM ATAT, respectively. It is seen that the current of Al in NaCl solution alone, curve 1, recorded very low values compared to that obtained after 60 min immersion, Fig. 2, curve 1, before applying the constant potential. It is well known that the uniform corrosion of metals and alloys starts with a high rate then slows with time due to the formation then accumulation of the corrosion products on the corroded surfaces. Here, elongating the immersion time of Al in the chloride solution allowed its surface to develop a thick layer of Al_2O_3 and/or the accumulation of corrosion products that led to the decrease of the measured current. These values of current further decreased with increasing the time of the applied potential till the end of the run. In the presence of ATAT, curve 2, the current recorded much lower values from the first moment of applying the constant potential confirming that ATAT molecules provided more protection for the aluminum surface. However, there is no indication that Al shows any pitting corrosion either ATAT is there or not. This might be due to immersing Al for long time in the tested solutions shifted its pitting potential to a value that is less negative than -680 mV vs. Ag/AgCl. The

current-time behavior thus confirms the data obtained from polarization ones both indicate that ATAT can be used as a corrosion inhibitor for Al in 3.5 wt.% NaCl solutions.

3.3. Electrochemical impedance spectroscopy (EIS) measurements

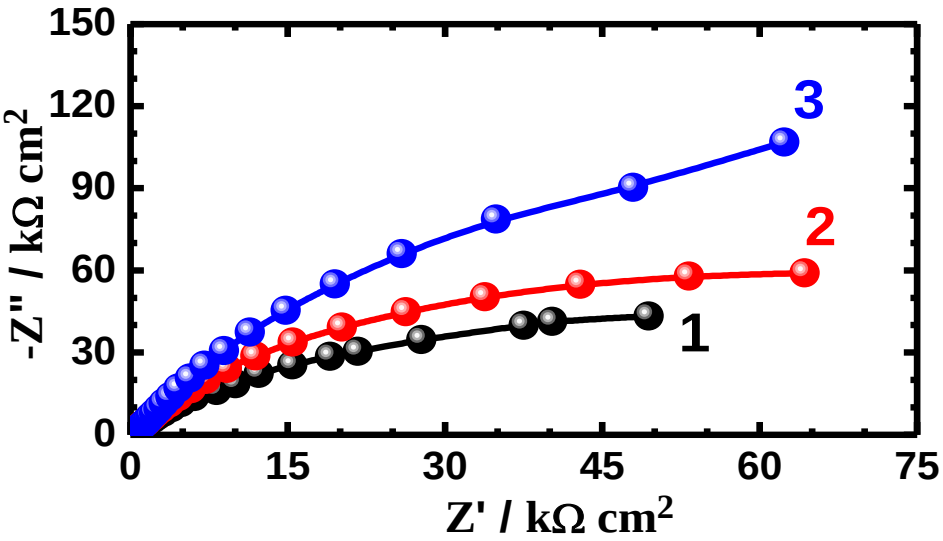

Figure 4. Typical Nyquist plots obtained for aluminum electrode at the corrosion potential after 60 min immersion in aerated stagnant 3.5 wt.% NaCl containing (1) 0.0 mM, (2) 1.0 mM, and (3) 5.0 mM ATAT, respectively.

Figure 4 shows typical Nyquist plots obtained for aluminum electrode after 60 min immersion in aerated stagnant 3.5 wt.% NaCl solution containing (1) 0.0 mM, (2) 1.0 mM, and (3) 5.0 mM ATAT, respectively. The EIS data shown in the figure were analyzed by fitting it to the equivalent circuit model shown in Fig. 5. This circuit was used before in the fitting of EIS data obtained in studying the inhibition of aluminum corrosion in sodium chloride solutions at similar conditions [2]. The EIS parameters obtained by fitting the equivalent circuit shown in Fig. 5 are listed in Table 2. Where, R_S is the solution resistance, Q_1 the constant phase elements (CPEs), Q_2 another constant phase elements, R_{P1} the polarization resistance and can be defined as the charge transfer resistance of the cathodic reduction reaction of Al, R_{P2} another polarization resistance, and W the Warburg impedance [42].

It is clear from Fig. 4 that only single semicircles are observed for the Al electrode in the chloride solutions regardless of whether ATAT is present or not. The chord length pertaining to the high frequency (HF) loop observed in Nyquist diagram related to NaCl, curve 1, is small and gets wider in the presence and the increase of ATAT concentration. At this condition, the semicircles at HF are generally associated with the relaxation of the capacitors of electrical double layers with their diameters representing the charge transfer resistances [42-48]. This is due to the decrease of the electrochemical active and flawed areas on the aluminum surface by both stabilizing the formed oxide film and the adsorption of ATAT molecules on Al. The diameter of the semicircle for Al at low

frequency (LF) also increases upon the addition and the increase of ATAT concentration as can be seen by curve 2 and curve 3 of Fig. 4.

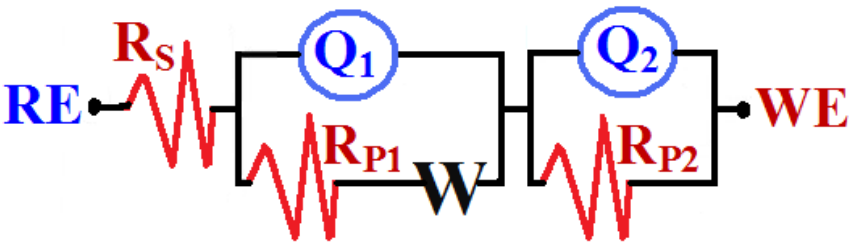

Figure 5. The equivalent circuit used to fit the experimental data presented in Fig. 4.

Table 2 showed that the values of R_S, R_{P1} and R_{P2} for Al in 3.5% NaCl solutions increased in the presence of ATAT and by the increase of its concentration. This is due to the decrease of Al corrosion by the adsorbed ATAT layer on its surface, which also makes the oxide film more resistant to chloride ions attack. The constant phase elements (CPEs), Q_1 and Q_2 with their n-values above 0.5 and more close to 1.0 represent double layer capacitors with porous structures on the surface. The CPE at this condition has been reported earlier [49] to be defined according to the following relation;

$$Z(CPE) = \left(\frac{Y_0 \text{-} 1}{(j\omega)^n} \right) \qquad (8)$$

Where, Y0 is the CPE constant, ω is the angular frequency (in rad s^{-1}), $j^2 = -1$ is the imaginary number and n is the CPE exponent. Depending on the value of n, CPE can represent resistance (Z(CPE) = R, n = 0), capacitance (Z(CPE) = C, n = 1) or Warburg impedance for (n = 0.5).

Table 2. EIS parameters obtained by fitting the Nyquist plots shown in Fig. 4 with the equivalent circuit shown in Fig. 5 for the aluminum electrode in aerated stagnant 3.5 wt.% NaCl solutions.

Solutions	Parameters								
	R_S / Ω cm^2	Q_1		R_{P1} / kΩ cm^2	W / Ω $S^{-1/2}$	Q_2		R_{P2} / kΩ cm^2	IE / %
		Y_{Q1} / μF cm^{-2}	n			Y_{Q2} / μF cm -2	N		
3.5 wt.% NaCl	9.89	11.62	0.81	10.58	4.8x10-5	0.392	1.0	14.89	–
+ 1.0 mM ATAT	14.33	11.04	0.87	37.14	6.7x10-6	0.298	0.58	19.15	71.7
+ 5.0 mM ATAT	21.81	11.03	0.89	52.17	5.4x10-6	0.167	0.68	24.3	79.8

The decrease of the CPEs especially in presence of ATAT and the increase of its content suggests that the charged surfaces are covered with an adsorbed layer of the organic compound. The presence of the Warburg (W) impedance limits the surface reaction by mass transport. The values of IE% were calculated from EIS measurements as reported in our previous work [50-55] recorded circa 72% for 1.0 mM ATAT increased to about 80% when the concentration of ATAT was increased to 5.0 mM. This reveals that ATAT is a powerful corrosion inhibitor for Al in 3.5 wt.% NaCl solutions and its ability increases with the increase of its concentration.

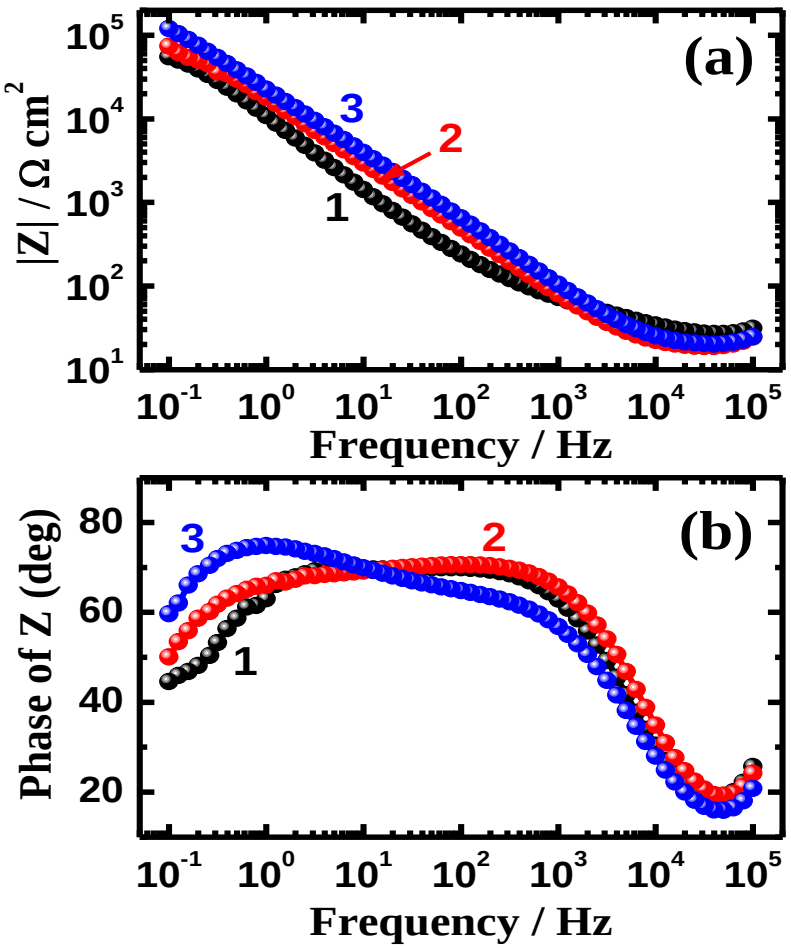

Figure 6. Bode impedance (a) and phase angle (b) plots for aluminum at the corrosion potential (EOCP ± 5 mV) after 60 min immersion in aerated stagnant 3.5 wt.% NaCl containing (1) 0.0 mM, (2) 1.0 mM, and (3) 5.0 mM ATAT, respectively.

Figure 6 shows the Bode impedance (a) and phase angle (b) plots obtained for aluminum at the corrosion potential after 60 min immersion in aerated stagnant 3.5 wt.% NaCl containing (1) 0.0 mM, (2) 1.0 mM, and (3) 5.0 mM ATAT, respectively. It can be seen from Fig. 8a that the impedance, |Z|, for aluminum electrode in the chloride solution alone, curve 1, shows the lowest values over the whole frequency range. The presence of 1.0 mM ATAT, Fig. 6a, curve 2, significantly raised the impedance values for Al over the whole frequency range. This effect increases with increasing the concentration

of ATAT to 5.0 mM. It has been reported [56] that the increase of the aluminum impedance value at the low frequency values is due to the high passivation of the surface against corrosion. This proves the hypothesis that ATAT inhibits the corrosion of Al through the adsorption of its molecules onto the Al surface to enhance the surface aluminum oxide film and prevent the formation of aluminum chloride and oxychloride complexes. This was also confirmed by plotting the degree of phase angle against frequency as seen in Fig. 6b. It can be seen from the curves of Fig. 6b that the maximum phase angle increase in the presence of ATAT and upon the increase of its concentration, which indicates on the inhibition of Al corrosion by ATAT.

4. CONCLUSIONS

The effects of 3-amino-1,2,4-triazole-5-thiol (ATAT) on the inhibition of aluminum corrosion after 60 min immersion in aerated stagnant 3.5 wt.% NaCl solution as a corrosion inhibitor have been reported using a variety of electrochemical and spectroscopic techniques. Cyclic polarization measurements indicated that the addition of ATAT to the chloride solution decreases the cathodic, anodic, corrosion, and passivation currents, and the corrosion rate, while increases the polarization resistance for Al and shifts the corrosion and pitting potential of Al towards the less negative values. Potentiostatic current-time experiments at -680 mV vs. Ag/AgCl showed that ATAT molecules decreased the absolute currents for Al. Electrochemical impedance spectroscopy data proved that the presence of ATAT increases the solution and polarization resistances of Al in the chloride solution. ATAT molecules not only repair the flawed areas on the oxide film that is formed on Al but also prevent the formation of the soluble aluminum chloride and oxychloride complexes and thus preclude the corrosion of Al in the corrosive NaCl solutions due to ATAT adsorption onto the surface. All measurements were in good agreement and confirmed that the increase of ATAT concentration decreases the corrosion of Al as a result of the increased inhibition efficiency of ATAT with its concentration.

ACKNOWLEDGEMENTS
The author extends his appreciation to the Deanship of Scientific Research at KSU for funding the work through the research group project No. RGP-VPP-160.

References

1. E.M. Sherif, S.-M. Park, *J. Electrochem. Soc.*, 152 (2005) B205.
2. E.M. Sherif, S.-M. Park, *Electrochim. Acta*, 51 (2006) 1313.
3. W.R. Osório, N. Cheung, L.C. Peixoto, A. Garcia, *Int. J. Electrochem. Sci.*, 4 (2009) 820.
4. El-Sayed M. Sherif, A.A. Almajid, F.H. Latif, H. Junaedi, *Int. J. Electrochem. Sci*., 6 (2011) 1085.
5. W. Diggle, T.C. Downie, C. Goulding, *Electrochim. Acta*, 15 (1970) 1079.
6. A.Y. El-Etre, *Corros. Sci*., 45 (2003) 2485.
7. L. Young, Anodic Oxide Films, Academic Press, New York, 1961, pp. 4-9.
8. F.H. Latief, El-Sayed M. Sherif, A.A. Almajid, H. Junaedi, *J. Anal. Appl. Pyrolysis*, 92 (2011) 485.

9. El-Sayed M. Sherif, E.A. El-Danaf, M.S. Soliman, A.A. Almajid, *Int. J. Electrochem. Sci*., 7 (2012) 2846.
10. C.M. A. Brett, *J. Appl. Electrochem*., 20 (1990) 1000.
11. C.M.A. Brett, I.A.R. Gomes, J.P.S. Martins, *Corros. Sci*., 36 (1994) 915.
12. S. Zein El Abedin, *J. Appl. Electrochem*., 31 (2001) 711.
13. P. M. Natishan, E. McCafferty, G. K. Hubler, *J. Electrochem. Soc*., 135 (1988) 321.
14. S.B. Saidman, J.B. Bessone, *J. Electroanal. Chem*., 521 (2002) 87.
15. N.A. Ogurtsov, A.A. Pud, P. Kamarchik, G.S. Shapoval, *Synth. Met*., 143 (2004) 43.
16. I.B. Obot, N.O. Obi-Egbedi, *Int. J. Electrochem. Sci*., 4 (2009) 1277.
17. A.Y. El-Etre, *Corros. Sci*., 43 (2001) 1031.
18. El-Sayed M. Sherif, R.M. Erasmus, J.D. Comins, *J. Electrochim. Acta*, 55 (2010) 3657.
19. El-Sayed M. Sherif, R.M. Erasmus, J.D. Comins, *J. Colloid Inter. Sci*., 306 (2007) 96.
20. El-Sayed M. Sherif, A.A Almajid, *J. Appl. Electrochem*., 40 (2010) 1555.
21. El-Sayed M. Sherif, *Int. J. Electrochem. Sci*., 7 (2012) 1482.
22. El-Sayed M. Sherif, *Int. J. Electrochem. Sci*., 7 (2012) 1884.
23. El-Sayed M. Sherif, R.M. Erasmus, J.D. Comins, *J. Colloid Interface Sci*., 311 (2007) 144.
24. El-Sayed M. Sherif, R.M. Erasmus, J.D. Comins, *J. Appl. Electrochem*., 39 (2009) 83.
25. El-Sayed M. Sherif, R.M. Erasmus, J.D. Comins, *Corros. Sci.*, 50 (2008) 3439.
26. El-Sayed M. Sherif, S.-M. Park, *Electrochim. Acta*, 51 (2006) 6556.
27. El-Sayed M. Sherif, S.-M. Park, *Corros. Sci*., 48 (2006) 4065.
28. El-Sayed M. Sherif, *Appl. Surf. Sci*., 252 (2006) 8615.
29. A.M. Shams El Din, M.E. El Dahshan, A.M. Taj El Din, *Desalination*, 130 (2000) 89.
30. El-Sayed M. Sherif, R.M. Erasmus, J.D. Comins, *J. Colloid Inter. Sci*., 309 (2007) 470.
31. El-Sayed M. Sherif, J.H. Potgieter, J.D. Comins, L. Cornish, P.A. Olubambi, C.N. Machio, *Corros. Sci.*, 51 (2009) 1364.
32. El-Sayed M. Sherif, A.H. Ahmed, Synthesis and Reactivity in Inorganic, *Metal-Organic, and Nano-Metal Chemistry*, 40 (2010) 365.
33. El-Sayed M. Sherif, *Int. J. Electrochem. Sci*., 6 (2011) 1479.
34. El-Sayed M. Sherif, *Int. J. Electrochem. Sci*., 7 (2012) 2374.
35. El-Sayed M. Sherif, *Int. J. Electrochem. Sci*., 6 (2011) 2284.
36. El-Sayed M. Sherif, *J. Solid State Electrochem*., 16 (2012) 891.
37. Z. Szklarska-Smialowska, *Corros. Sci*., 41 (1999) 1743.
38. N. Sato, *Corros. Sci*., 37 (1995) 1947.
39. R.T. Foley, T.H. Nguyen, *J. Electrochem. Soc.*, 129 (1982) 464.
40. F. Hunkeler, G.S. Frankel, H. Bohni, *Corrosion* (NACE), 43 (1987) 189.
41. I.Yamaguchi, T. Yamamoto, *React. Funct. Polymers*, 61 (2004) 43.
42. H. Ma, S. Chen, L. Niu, S. Zhao, S. Li, D. Li, *J. Appl. Electrochem*., 32 (2002) 65.
43. E.M. Sherif, S.-M. Park, *J. Electrochim. Acta*, 51 (2006) 4665.
44. K.A. Khalil, El-Sayed M. Sherif, A.A. Almajid, *Int. J. Electrochem. Sci*., 6 (2011) 6184.
45. El-Sayed M. Sherif, *Int. J. Electrochem. Sci*., 6 (2011) 3077.
46. El-Sayed M. Sherif, *Int. J. Electrochem. Sci*., 6 (2011) 5372.
47. El-Sayed M. Sherif, A.A. Almajid, A.K. Bairamov, Eissa Al-Zahrani, *Int. J. Electrochem. Sci*., 6 (2011) 5430.
48. El-Sayed M. Sherif, J.H. Potgieter, J.D. Comins, L. Cornish, P.A. Olubambi, C.N. Machio, *J. Appl. Electrochem.*, 39 (2009) 1385.
49. Z. Zhang, S. Chen, Y. Li, S. Li, L. Wang, *Corros. Sci*., 51 (2009) 291.
50. El-Sayed M. Sherif, A.A. Almajid, A.K. Bairamov, Eissa Al-Zahrani, *Int. J. Electrochem. Sci*., 7 (2012) 2796.
51. El-Sayed M. Sherif, *Int. J. Electrochem. Sci*., 7 (2012) 2832.
52. El-Sayed M. Sherif, *Int. J. Electrochem. Sci*., 6 (2011) 2131.

53. El-Sayed M. Sherif, *Mater. Chem. Phys*., 129 (2011) 961.
54. El-Sayed M. Sherif, *J. Mater. Eng. Perform*., 19 (2010) 873.
55. El-Sayed M. Sherif, *Int. J. Electrochem. Sci*., 7 (2012) 4235.
56. F. Mansfeld, S. Lin, S. Kim, H. Shih, *Corros. Sci*., 27 (1987) 997.